AJNR

MR imaging of intracranial cysticercosis: comparison with CT and anatomopathologic features.

R A Suss, K R Maravilla and J Thompson

AJNR Am J Neuroradiol 1986, 7 (2) 235-242
http://www.ajnr.org/content/7/2/235

MR Imaging of Intracranial Cysticercosis: Comparison with CT and Anatomopathologic Features

Richard A. Suss[1]
Kenneth R. Maravilla[1]
James Thompson[2]

Eight patients with neurocysticercosis were studied with CT and magnetic resonance (MR) imaging. Two cysts were shown better with MR than with CT. A conspicuous, high-intensity mural nodule containing the scolex allowed specific identification of intraventricular and parenchymal cysticerci. CT evidence of calcification and metrizamide enhancement in the nodule was also noted in one case. Racemose cysts were seen in the cerebellopontine angle and under the anterior septum pellucidum. Fluid in apparently live cysticerci and in racemose cysts had MR signal properties closely paralleling CSF. A thin subependymal or subpial rim of high signal intensity around the intraventricular and one of the racemose cysts was consistent with tissue reaction and aided diagnosis. While MR showed only one of numerous calcifications, it may be more sensitive than CT in the recognition of perifocal edema and of parenchymal and subarachnoid cysts, may replace invasive ventriculography in the diagnosis of intraventricular cysts, and may be useful in determining the viability of cysts and their response to therapy.

Neurocysticercosis is an infestation of the central nervous system by larvae of *Taenia solium*, the pork tapeworm. Fecal shedding of eggs by the definitive host, man, contaminates the soil, fingers, etc., leading to ingestion of eggs by an intermediate host such as the pig, or man. The primary larvae, oncospheres, hatch in the intestine and are distributed hematogenously to brain and other tissues, where they develop into secondary larvae, cysticerci [1].

Significant human morbidity caused by dead larvae includes seizures, intracranial hypertension, basal arachnoiditis, focal neurologic deficits, and dementia [2–7]. Cysticercosis is the most common identifiable cause of seizures in young adults in endemic areas [8]. Intracranial hypertension can be caused by degenerating larvae that provoke extensive cerebral edema or cause cerebrospinal fluid (CSF)-pathway obstruction due to arachnoiditis or ependymitis, as well as by live larvae that block the ventricular system or are present in large numbers in the brain parenchyma [7].

Immunologic studies on CSF or serum and abnormal CSF findings such as protein elevation, glucose depression, or eosinophilia may support the diagnosis of cysticercosis, but these tests are often insensitive and nonspecific [1–3, 5, 8–10]. Radiologic studies are the most sensitive and commonly most specific diagnostic tests [11–14], especially with the availability of computed tomography (CT) of the brain, the most commonly affected organ [1, 2]. Accurate diagnosis, especially the recognition of live cysts, has acquired new significance with the possibility of effective chemotherapy using praziquantel [15]. The cysticercus with its spherical wall, fluid contents, and nodular "scolex," is potentially recognizable by magnetic resonance (MR) [16]. This study was undertaken to compare CT and MR findings and to investigate the potential for MR diagnosis of cysticercosis.

Subjects and Methods

Eight patients of Mexican origin with neurologic complaints and CT findings suggesting

Received May 7, 1985; accepted after revision August 6, 1985.

Presented at the annual meeting of the American Society of Neuroradiology, New Orleans, February 1985.

[1] Department of Radiology, University of Texas Health Science Center, 5323 Harry Hines Blvd., Dallas, TX 75235. Address reprint requests to R. A. Suss.

[2] Department of Neurology, University of Texas Health Science Center, Dallas, TX 75235.

***AJNR* 7:235–242, March/April 1986**
0195–6108/86/0702-0235

TABLE 1: **Summary of Clinical, Laboratory, and Imaging Data**

	Case No.							
	1	2	3	4	5	6	7	8
Demographic data:								
Age	42	23	41	45	63	50	53	17
Time in USA (months)	N	48	3	12	120	2	60	60
Clinical findings:								
Seizures	+	−	--	−	+	+	+	+
Headaches	−	+	+	+	−	−	−	+
Other neurologic complaints	−	+	+	+	−	−	−	+
Papilledema or elevated ICP	−	−	+	+	+	−	−	−
Laboratory findings:								
CSF eosinophilia	N	+	+	+	N	+	−	−
CSF cysticercus titer >1:4	N	+	N	−	N	−	−	−
Serum cysticercus titer >1:32	N	+	N	−	N	−	−	−
Imaging findings:								
Cerebral Ca^{++} on CT	+	−	−	−	+	+	+	+
Cerebral Ca^{++} (black) on MR	−	−	−	−	+	−	−	−
Edema on initial CT	−	−	−	−	+	+	+	+
Edema on initial MR	−	+	−	−	+	+	+	−
Enhancement (CT)	+	+	−	−	+	+	+	−
Hydrocephalus (CT and MR)	−	+	+	−	+	−	−	−
Cyst on initial CT	?	+/?*	−	+	−	−	−	−
Cyst on initial MR	+	+/+*	−	+	−	−	−	−

Note.—N = information not available; ICP = intracranial pressure; CSF = cerebrospinal fluid; ? = doubtful (case 1) or not recognized prospectively (case 2).

* Two cysts.

cysticercosis were studied with MR. Clinical, laboratory, and imaging findings supporting the diagnosis of cysticercosis are summarized in table 1. Serology consisted of indirect hemagglutination (IHA) titers analyzed at the Centers for Disease Control in Atlanta. Significant additional or corroborative findings were made with MR in five patients (cases 1–5).

Spin-echo (SE) MR imaging was performed on a Diasonics MT/S 0.35 T superconducting system [17]. Multislice sequences with short (0.5 sec) and long (1.5 or 2.0 sec) repetition times (TR) were performed using 28 and 56 msec echoes. Axial, coronal, and sometimes sagittal images were obtained. The slice thickness was 7 mm with 3 mm interslice gaps. Images were acquired on a 128 × 128 matrix with a 1.7 mm pixel size and were interpolated to a 256 × 256 matrix for display. MR findings were compared with CT findings from GE 8800 scanners.

Representative Case Reports

Case 1

A 42-year-old woman was examined because of a seizure disorder. CT showed several 3–6 mm calcifications in the left cerebral hemisphere. MR (fig. 1) showed a round cyst 1 cm in diameter near the left parietal vertex, having signal slightly greater than CSF and containing a 3 mm high-signal mural nodule. In retrospect, an arcuate density seen on contrast-enhanced CT may have represented part of the cyst wall, but was indistinguishable from a cortical vein.

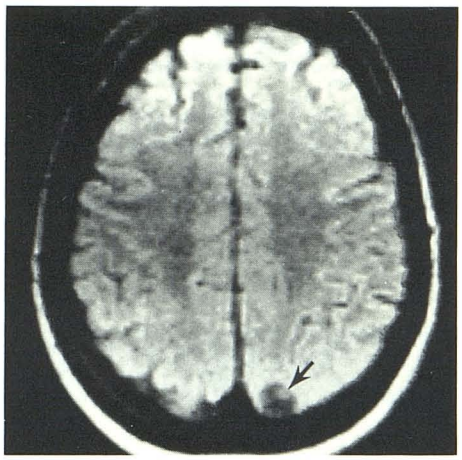

Fig. 1.—Case 1. SE 1500/28 image. Cysticercus is 1 cm round low-signal area with 3 mm eccentric high-signal mural nodule (*arrow*) containing scolex.

Case 2

A 23-year-old woman had a 1 day history of headache, lethargy, confusion, nausea, and vomiting. She was afebrile, with slight nuchal rigidity, no papilledema, and a 3% peripheral eosinophilia. Serum IHA titers for cysticercosis were 1:128 and 1:256. Lumbar opening pressure was normal. There was a CSF pleocytosis with 95% mononuclear cells and 1%–4% eosinophils. A technetium brain scan showed focal uptake in the right parietal vertex.

Intravenously enhanced CT after unenhanced CT showed a 13 × 8 mm thin ring enhancement with a 2 mm dense, enhancing mural nodule. The contents of the ring were otherwise of approximately CSF density, and there was no evidence of surrounding edema (fig. 2A). The third and lateral ventricles, including the temporal horns, were mildly to moderately enlarged. The anterior part of the third ventricle was disproportionately widened. Just behind the middle of the third ventricle and closer to the right lateral wall there was a 2 mm nodule whose apparent density on a 10 mm unenhanced cut was similar to gray matter (fig. 2B). This nodule was less easily appreciated on the contrast-enhanced scan, probably because of adjacent blood vessels and choroid plexus.

MR 7 days later showed a high-signal, long-T2 abnormality (edema) in a 2–3 cm diameter volume of right parietal white matter. A parenchymal cysticercus within this region was imaged only on the short-TR sequences as a 7 mm cyst with a 2 mm mural nodule (fig. 2C). A 10 × 8 mm oval cyst containing a 4 mm mural nodule was shown in the third ventricle (figs. 2D and 2E). The ventricular cyst fluid had slightly higher signal than did CSF. The mural nodule had a longer T2 than did gray or white matter. Surrounding the third and lateral ventricles there was a high-signal, 3 mm rim with prolonged T2 compared with normal brain tissue. Confirmation of the third ventricular cyst was obtained by metrizamide ventriculography (fig. 2F).

One week after start of praziquantel therapy repeat CT showed further widening of the third ventricle suggesting swelling of the cyst, while the lateral ventricles were unchanged. Repeat MR 3 weeks after the start of therapy showed enlargement of the third ventricular cyst to 14 × 10 mm on coronal images. There was no further enlargement of the lateral ventricles, and the periventricular high-signal rim was reduced. The right parietal white-matter signal was

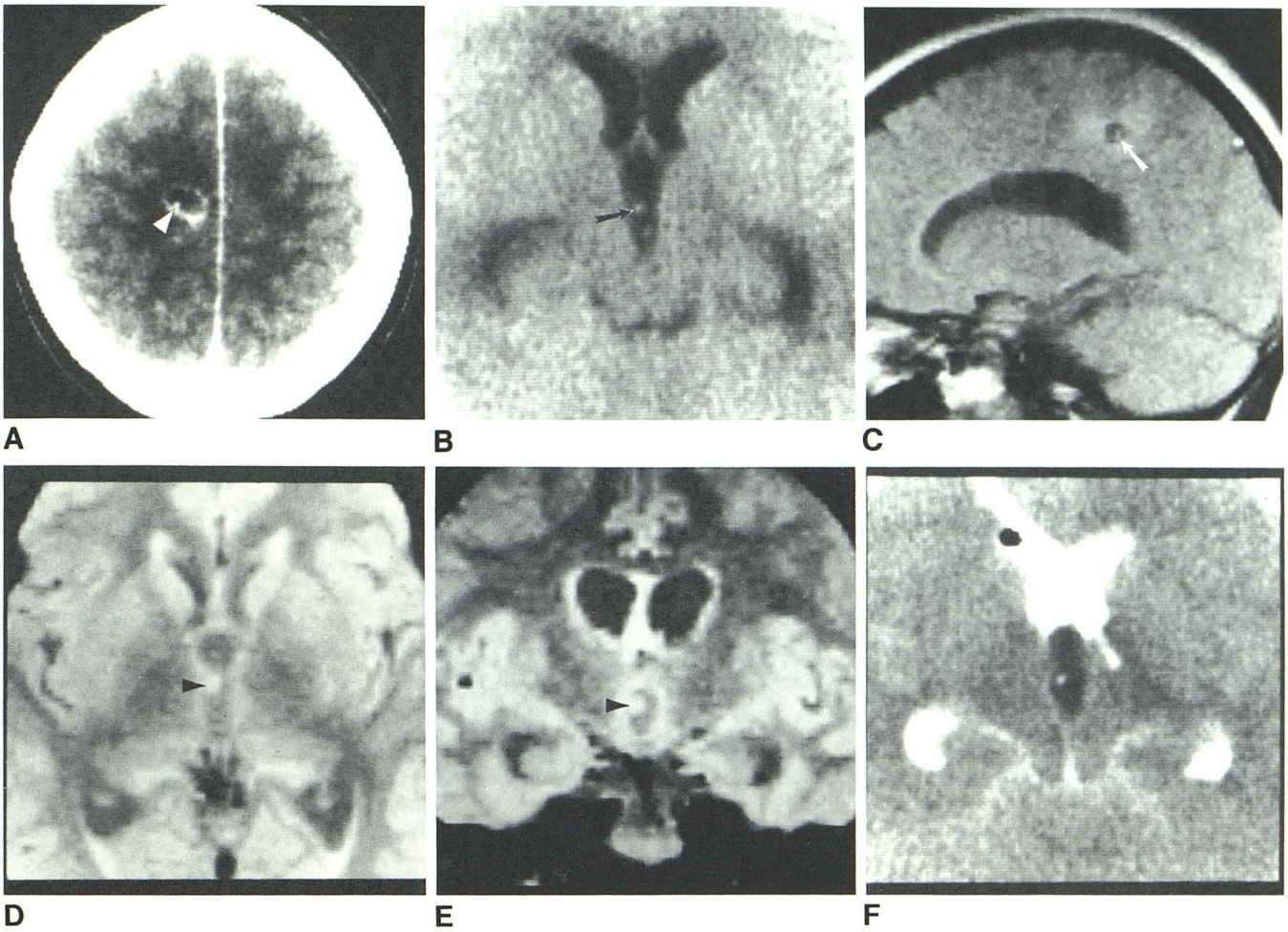

Fig. 2.—Case 2. **A**, Intravenously enhanced CT scan shows 1 cm parietal lucency with thin, enhanced rim and mural nodule (*arrowhead*). **B**, Unenhanced CT scan. Mild ventriculomegaly, disproportionate enlargement of anterior third ventricle, and 2 mm nodule within third ventricle (*arrow*). **C–E**, MR 7 days later but before praziquantel therapy. **C**, Sagittal SE 500/56 scan. Cyst, nodule (*arrow*), and edema in right parietal lobe. Axial SE 2000/28 (**D**) and coronal SE 1500/56 (**E**) images show nodule (*arrowheads*) lying eccentrically in cyst in inferior third ventricle. Above interthalamic adhesion, third ventricle is narrow. **F**, Metrizamide ventriculogram confirms nonobstructing cyst within third ventricle. Nodule appeared denser than in **A**, suggesting metrizamide penetration.

normal and no parenchymal cyst could be detected on long- or short-TR sequences. CT the next day showed a nearly solid, 6 × 8 mm enhancement in the right parietal lobe without surrounding edema.

Case 3

A 41-year-old woman had a 1.5 year history of tinnitus, vertigo, decreased hearing in the left ear, and intermittent paresthesias of the left side of the tongue; a 10 month history of total left facial paralysis; and recent onset of headache. She had a complete peripheral left facial nerve paralysis, decreased sensation in all three divisions of the left trigeminal nerve, and bilateral papilledema with retinal flame hemorrhages. There was an unexplained secondary (low erythropoietin) erythrocytosis with hematocrits of 60%–65%. CT (figs. 3A and 3B) showed a widened left internal auditory canal (IAC) without evidence of a mass but with apparent widening of the cerebellopontine (CP) angle and medullary cisterns. A linear density crossing the CP angle cistern (fig. 3B) was thought to represent a stretched blood vessel or enhancement of the seventh and eighth nerve bundle stretched slightly cephalad to the IAC. There was no abnormal contrast enhancement of the brainstem or cerebellum. The third and lateral ventricles were moderately to markedly enlarged but the fourth ventricle was normal. MR (figs. 3C and 3D) confirmed the widened IAC and showed a high-signal focus laterally within it. Cisternal widening was also confirmed, with signal properties identical to CSF and no high-signal abnormality in the margins. At surgery the seventh and eighth nerve bundle was densely fibrotic. Beneath it a free-floating cystic mass was found in the CP angle and medullary cisterns that was identified pathologically as a "degenerated larval cyst of *Taenia solium*."

Case 4

A 45-year-old woman had a 8 hr history of severe, diffuse headache, with the development of nausea, vomiting, and dizziness. There had been a long history of less severe headaches, but a headache

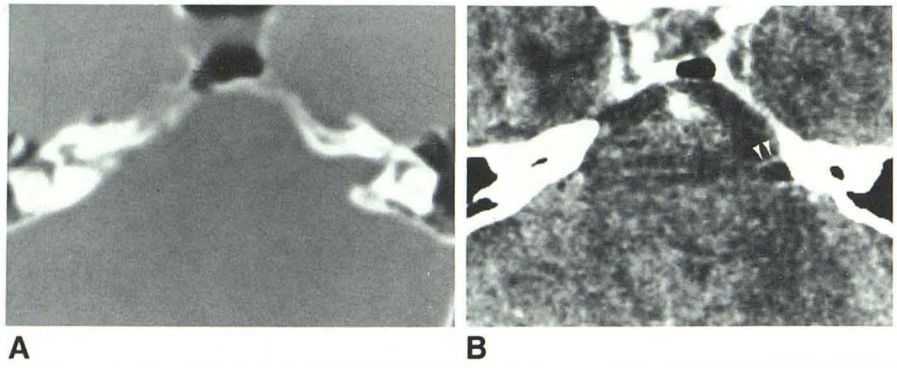

A B

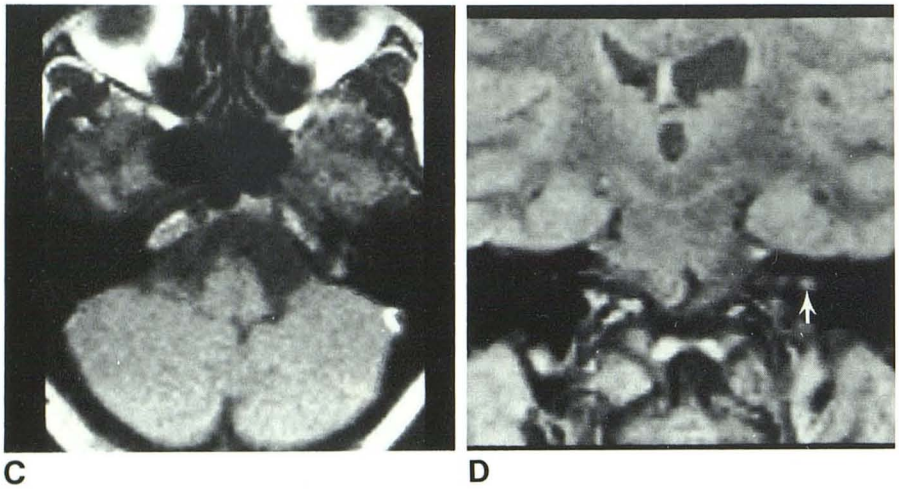

C D

Fig. 3.—Case 3. **A** and **B**, Intravenously enhanced CT scans, 1.5 mm slice thickness. Widened IAC and CP angle cistern. Stretched blood vessel or VII and VIII cranial nerve bundle (*arrowheads*) slightly above level of IAC. Axial SE 500/56 (**C**) and coronal SE 1500/56 (**D**) images show widened left CP angle and medullary cisterns and widened internal auditory canal containing high-signal focus (*arrow*). Signal properties of fluid within widened cistern are identical to those of CSF. No evidence of mass or tissue reaction. Surgically proven racemose cyst.

A B

Fig. 4.—Case 4. Axial SE 2000/56 (**A**) and coronal SE 500/28 (**B**) images. Cyst originating in cistern of lamina terminalis and displacing septum pellucidum upward. Prominent high-signal rim in **A** represents tissue reaction to cyst.

similar to the present one occurred 6 years earlier. She also complained of occasional right hand and face paresthesias. Physical examination was normal. Lumbar opening pressure was 47 cm H_2O. CSF glucose was 33 mg/dl (serum 103); protein was 61–81 mg/dl; red blood cell count, 10–350/mm^3; white blood cell count, 40–1165/mm^3, with 4%–14% neutrophils, 44%–48% lymphocytes, 17%–29% monocytes, and 4%–39% eosinophils (lumbar puncture performed twice). CT showed a 2.5 × 1.5 cm cyst apparently in the inferior part of the septum pellucidum, without edema or abnormal contrast enhancement. MR 5 days later (fig. 4) showed that the cyst lay under the septum pellucidum, originating in the cistern of the lamina terminalis and pushing the septum up. The cyst fluid had signal properties identical to CSF and contained no mural nodule. Long-TR sequences showed the cyst surrounded by a high-signal, 3 mm rim, with prolonged T2 compared with normal brain tissue. The patient refused therapy and returned to Mexico.

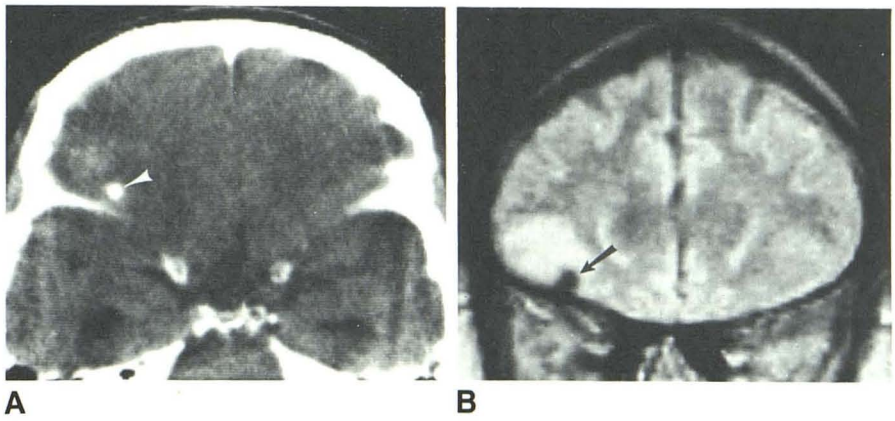

Fig. 5.—Case 5. **A**, Unenhanced CT scan shows 4 mm calcification (*arrowhead*) just above right sphenoid wing. Higher section (not shown) showed white matter edema. **B**, SE 1500/56 scan 4 weeks later shows 6 mm area of absent signal (*arrow*) corresponding in location to CT calcification. Surrounding zone of abnormal high signal represents edema corresponding predominantly to orbitofrontal gray matter.

Case 5

A 63-year-old man presented with new onset of seizures, having focal onset in the left arm and subsequent generalization. Physical examination was remarkable only for postictal effects and for papilledema. CT showed moderate hydrocephalus, numerous calcifications in the choroid plexus or the walls of the third and left lateral ventricles, and scattered parenchymal and sulcal calcifications. The largest calcification measured 4 mm and was located just above the right lesser sphenoid wing, surrounded by poorly defined lucency (edema) in the inferior frontal white matter (fig. 5A). There was no abnormal contrast enhancement. MR 4 weeks later (fig. 5B) showed abnormally high signal (edema) in the right orbitofrontal gray matter. Within this area was a 6 mm zone of absent signal on all sequences, corresponding to the location of the calcification. None of the other calcifications could be appreciated.

Discussion

Cysticerci

The cysticercus is a vesicular (bladder) larva ranging from 5 mm to 2 cm, less commonly up to 4 cm, in diameter [18, 19]. The most typical size is about 1 cm. It develops from the oncosphere by the envelopment of the solid larva within a cyst growing from the caudal end of the organism (hence, *cysticercus*, meaning *bladder tail*). Thus the parenchymatous region containing the scolex is transformed into an invagination of the cyst wall. In the fully developed cysticercus this region forms a round nodule measuring 2–3 mm, sometimes up to 5 mm, in diameter. The nodule contains the scolex at the inner end of a spiral canal that joins with a vestibule to reach the cyst's surface through an entrance canal. Numerous calcareous corpuscles (physiologic structures of calcium carbonate unrelated to later pathologic calcification [20]) are closely packed along the spiral canal in the neck of the organism [11, 21]. The scolex proper is only 1 mm in diameter [1], although for convenience the entire mural nodule is sometimes called the scolex. The cyst wall is 0.07–0.1 mm thick [22]. The cyst fluid has been described as transparent in live cysts, turning turbid or "jellylike" with the death of the organism [23–25]. There would not seem to be much taenial protein antigen in the cyst fluid because fluid spilled at surgery is not necessarily harmful to the patient [26, 27]. Related cestode larvae have been shown to take up host albumin and immunoglobulins while alive [28], but the quantitative significance for cysticerci is unknown. Explicit measurements of the protein content per unit volume of fluid for direct comparison with CSF are not available.

This biologic description provides a basis for several CT and MR observations. The parenchymal and ventricular cysticerci (as opposed to the cisternal racemose cysts) were all about 1 cm in diameter and each contained a 2–4 mm mural nodule, producing a characteristic "hole-" or "ring-with-eccentric-dot." Metrizamide may have penetrated the channels in the nodule of the intraventricular cysticercus (fig. 2F). The thin wall of the cyst was not imaged per se on CT or MR, and could only be inferred from the sharp, smooth outline of the cyst fluid or from the pattern of ventricular or cisternal distortion. The configuration of a ring or arcuate calcification around a 2–5 mm solid calcification on skull films has long been recognized as highly suggestive if not conclusive evidence of cysticercosis [3, 12, 18, 29, 30]; the analogous configuration of live and early degenerating cysticerci now imaged with CT [7, 10, 16] and MR should prove at least as specific.

The significance of the calcareous corpuscles is suggested by two observations. Considering the effect of volume-averaging, the nodules of the cysticerci seen on unenhanced CT in this study (case 2) were surprisingly dense. Their intrinsic density may have been greater than that of brain because of these calcifications. Moreover, in the one apparently live cysticercus that was well seen on both CT and MR, the nodule appeared smaller on CT (about 2 mm in fig. 2B) than on MR (4 mm in fig. 2D). This difference in the imaged sizes may have resulted from a difference in what is imaged by the two methods. CT shows calcifications to best advantage, emphasizing the central region of calcareous corpuscles concentrated along the spiral canal, but poorly distinguishing the more peripheral part of the nodule from the surrounding fluid. MR sensitivity to the difference between fluid water and tissue water causes the entire volume of the nodule to be imaged clearly, making it larger, more conspicuous, and more convincing on MR compared with CT.

The fluid of the two probably live cysticerci appeared to have a slightly higher signal than CSF on long-TR images, while reliable comparison was not possible on the available short-TR images. This impression was confirmed by signal intensity measurements and relaxation time calculations in case 2. It becomes difficult, however, to obtain a valid CT density number or MR signal level for a lesion as its diameter perpendicular to the slice decreases below twice the slice thickness, and impossible below the slice thickness. Volume-averaging could explain the slightly increased MR signal as well as the reported slightly greater CT density [6] of cysticercal fluid compared with CSF. While we cannot exclude a slight increase in inherent signal level, it was not markedly increased compared with CSF.

If the reported turbidity and gelling of the fluid after cyst death [23–25] correlate with MR signal changes and if reliable measurements on cyst fluid can be made reasonably free of volume-averaging, signal measurements may help discriminate live from dying cysticerci. One cysticercus, thought to be dying as indicated by CT findings of marked contrast enhancement initially and subsequent solidification, was visible on short- but not long-TR sequences on the initial MR (fig. 2C). This MR finding may have resulted from increased signal intensity (compared with CSF) of the cyst fluid on long-TR sequences, caused by elevated or otherwise altered protein content, bringing the cysticercus sufficiently close to isointensity with brain on these images so that it was not discernible. Thus, while the best contrast between high-signal nodule and low-signal fluid in a live cyst may be found on a long-TR, short-TE image (e.g., SE 1500/28), a dying cyst's fluid may contrast very poorly against nodule and brain on long-TR images and may be perceived best or solely on a short-TR image. Such MR-derived information indicating cyst death would be useful in patient selection for and monitoring of therapy.

Parenchymal Cysticerci

Our own experience and that of others [10, 13, 14, 31] has indicated that the parenchyma is the most common location of CNS cysticerci. Many of those that appear intracortical on sectional images actually lie within the sulcal subarachnoid space, but the sum of sulcal and parenchymal cysts constitutes a majority of the organisms [19]. The propensity to involve the cortical (as well as deep) gray matter [4, 12, 25, 31, 32] and overlying leptomeninges places many cysts near the skull, which is a difficult area to examine by CT, with its attendant bone artifacts. The failure to detect by CT a superficial cyst that was easily identified by MR demonstrated an advantage for MR in detecting convexity cysts, particularly those near the vertex.

Host Reaction

Microscopically there is a thin host capsule of compressed tissue with slight gliosis and inflammation and sometimes a localized endarteritis around live cysticerci in the brain [1, 12, 19, 20, 32], but there is little or no radiologic evidence of host response [13–16, 33]. The lack of demonstrated response around cysts can produce a "Gruyere (Swiss) cheese" [13] or punched-out appearance in the brain parenchyma and surprisingly little distortion of neighboring structures [34]. This inert appearance may be found on MR (fig. 1) as well as CT. Paradoxically, a thin subependymal rim was seen on MR around the intraventricular cyst in case 2 when the organism was thought to be alive and was reduced during praziquantel therapy.

At the death of the organism, a more marked inflammatory response is found [1, 2, 33]. This accelerated inflammation may be the cause of the death of the organism [19], although it has usually been assumed to be the result. The dying cysticercus is ordinarily associated with contrast enhancement and edema on CT [15, 16, 33]. MR is at least as sensitive as CT for the detection of brain edema, optimally using SE sequences with long TR and long TE [35], and MR demonstration of cysticercotic edema has previously been illustrated [16]. For most of the patients in this study, too much time elapsed between CT and MR to permit a reliable comparison of detection of inflammatory phenomena. An MR contrast agent such as gadolinium-DTPA [36] would be useful to fill the role of CT contrast enhancement both in the recognition of early parasite death and in the detection of organisms in more advanced stages of involution such as the parenchymal parasite in case 2 that was invisible on the second MR examination.

The final development in the dead organism is calcification, usually beginning in the nodule [2, 3, 29] (among extracellular fibers, not the calcareous corpuscles [20]). Calcification has in our experience and that of others [37] been the most common CT manifestation of cysticercosis, but poor detection of calcification is a known weakness of MR. In case 5, only one of several calcifications was appreciable (fig. 5), while MR failed to detect any of the calcifications in cases 6–8.

Intraventricular Cysticerci

Detection of potentially life-threatening intraventricular cysts is important in the workup of neurocysticercosis. In the Los Angeles County series 46 patients (17%) had intraventricular cysts, and six patients died from acute ventricular obstruction [38]. Plain CT has been considered inadequate for diagnosis of intraventricular cysts [14, 16, 33, 37–44], although a lateral ventricular cyst has been shown directly without intraventricular contrast medium [45] and cysticercosis has been suspected on the basis of distortion or disproportionate enlargement of the third [38] or fourth [9, 16, 26, 44] ventricle. Ventricular synechiae caused by intraventricular cysts have been observed by pneumoencephalography [18] and need to be differentiated from the cysts themselves if surgical removal is contemplated.

Suspicion of the third-ventricular cyst on CT was based primarily on the presence of otherwise unexplained hydrocephalus; the significance of the mild anterior distortion of the third ventricle together with the eccentric nodular density was not recognized prospectively. The superiority of MR for initial intraventricular cyst detection resulted from the greater con-

spicuity of the scolex and from the ease of coronal imaging to better appreciate the nature of the ventricular distortion. The potential of MR to replace metrizamide CT ventriculography in selected cases is important not only for primary diagnosis but also because it may be necessary to reconfirm preoperatively the ventricular location of a known cyst, as these can migrate between ventricles [38, 40, 45].

Definitive cyst identification in the fourth ventricle, where most intraventricular cysticerci occur [4, 5, 23, 26, 38, 43], may prove difficult, especially on CT, because the ballooned ventricle is likely to conform to the cyst wall. On MR the mural nodule and a reactive rim of high signal may indicate the presence of a cyst. Because of the small size of the nodule, contiguous MR sections may be important to detect it. Fourth ventricular cysts can be racemose [19, 43], lacking a scolex, but would probably produce the high-signal rim. Fourth ventricular enlargement can also be produced by cysticercal arachnoiditis without a cyst within the ventricle [18], in which case no periventricular high-signal zone would be anticipated.

Racemose Cysts

The racemose cyst is a multilobular, nonviable cyst often several centimeters in size, lacking a scolex. It is the degenerated form to which a cysticercus in the basal subarachnoid space is transformed [1, 19, 32]. Although sterile, it may be "alive" in that it can grow by proliferation of its wall [19], and may therefore be amenable to praziquantel therapy. Evidence of chronic meningitis typically accompanies racemose cysts [1].

The CP angle and the suprasellar region are locations known to harbor racemose cysts. Several examples of cysticercal CP angle cysts, some with IAC erosion and with clinical presentations suggesting acoustic schwannoma, have been reported [4, 14, 16, 46–48]. Multiple cranial nerves in the vicinity of a cisternal cysticercal cyst may have inflammatory infiltrates among their fibers [19], which can explain the contrast-enhancement observed (fig. 3B). Cysticercal cysts have been reported beneath [42] and within [49] the septum pellucidum. In case 4 a high-signal rim surrounded the cyst, and strong clinical and laboratory evidence for a parasitic meningitis supported the diagnosis. The differential diagnosis for a cyst in the septal area includes ependymal, arachnoid, and neuroepithelial cysts and cystic tumors including craniopharyngioma [49]. Because the racemose cyst's fluid appears identical to CSF on CT and MR, its diagnosis may be suggested only by apparent focal cisternal widening, but a high-signal rim caused by adjacent tissue reaction, when present, will be an additional clue.

Conclusions

Cysticerci have a characteristic configuration on MR imaging, consisting of a low-intensity focus about 1 cm in diameter with signal properties closely paralleling ventricular CSF, and a high-intensity, 2–4 mm mural nodule containing the scolex. Racemose cysts are distinguished by their larger size and lack of a mural nodule. Dying or degenerated cysts and possibly some live cysts may be surrounded by a high-intensity rim of tissue reaction. MR and CT are currently complementary in detection of these and other features of cysticercosis. MR shows some cysts (convexity, ventricular) better than CT does, is probably more sensitive than CT to surrounding edema, and may show internal changes indicative of cyst death. CT is superior in demonstration of calcification and, until MR contrast agents are available, blood-brain barrier breakdown. Positive-contrast CT cisternography and CT ventriculography remain the most sensitive detectors of cysts in the CSF pathways, but are invasive and may not be necessary when MR is positive. MR may prove to be the optimal primary imaging technique for diagnosis of suspected cysticercosis and for monitoring therapy of cysts and edema.

ACKNOWLEDGMENTS

We thank Jacob Rosenstein and Fred G. Silva for surgical and pathologic correlation in case 3 and Virginia Vaughn and Jerry Cheek for photographic assistance.

REFERENCES

1. Marquez-Monter H. Cysticercosis. In: Marcial-Rojas R, ed. *Pathology of protozoal and helminthic diseases with clinical correlation.* Baltimore: Williams & Wilkins, **1971**:592–617
2. MacArthur WP. Cysticercosis as seen in the British army, with special reference to the production of epilepsy. *Trans R Soc Trop Med Hyg* **1933**;27:343–363
3. Dixon HBF, Hargreaves WH. Cysticercosis (*Taenia solium*): a further ten years' clinical study, covering 284 cases. *Q J Med* **1944**;13:107–121
4. Obrador S. Clinical aspects of cerebral cysticercosis. *Arch Neurol Psychiatry* **1948**;59:457–468.
5. Obrador S. Cysticercosis cerebri. *Acta Neurochir* (Wien) **1962**;10:320–364
6. Schnur JA, Richardson EP. Case records of the Massachusetts General Hospital: cysticercosis cerebri. *N Engl J Med* **1977**;297:773–780
7. Torrealba G, Del Villar S, Tagle P, Arriagada P, Kase CS. Cysticercosis of the central nervous system: clinical and therapeutic considerations. *J Neurol Neurosurg Psychiatry* **1984**;47:784–790
8. McCormick GF, Zee C-S, Heiden J. Cysticercosis cerebri: review of 127 cases. *Arch Neurol* **1982**;39:534–539
9. Bentson JR, Wilson GH, Helmer E, Winter J. Computed tomography in intracranial cysticercosis. *J Comput Assist Tomogr* **1977**;1:464–471
10. Byrd SE, Locke GE, Biggers S, Percy AK. The computed tomographic appearance of cerebral cysticercosis in adults and children. *Radiology* **1982**;144:819–823
11. Brailsford JF. Cysticercus cellulosae—its radiographic detection in the musculature and the central nervous system. *Br J Radiol* **1941**;14:79–93
12. Cardenas-y-Cardenas J. Cysticercosis of the nervous system. II. Pathologic and radiologic findings. *J Neurosurg* **1962**;19:635–640
13. Rodriguez-Carbajal J, Boleaga-Duran B. Neuroradiology of human cysticercosis. In: Flisser A, Willms K, Laclette JP, Larralde C, Ridaura C, Beltran F, eds. *Cysticercosis: present state of knowledge and perspectives.* New York: Academic, **1982**:139–162

14. Rodriguez-Carbajal J, Palacios E, Zee C-S. Neuroradiology of cysticercosis of the central nervous system. In: Palacios E, Rodriguez-Carbajal J, Taveras JM, eds. *Cysticercosis of the central nervous system.* Springfield, IL: Thomas, **1983**:101–143
15. Sotelo J, Escobedo F, Rodriguez-Carbajal J, Torres B, Rubio-Donnadieu F. Therapy of parenchymal brain cysticercosis with praziquantel. *N Engl J Med* **1984**;310:1001–1007
16. Enzmann DR. Imaging of infections and inflammations of the central nervous system: computed tomography, ultrasound, and nuclear magnetic resonance. New York: Raven, **1984**:103–127
17. Crooks L, Arakawa M, Hoenninger J, et al. Nuclear magnetic resonance whole-body imager operating at 3.5 kGauss. *Radiology* **1982**;143:169–174
18. Santin G, Vargas J. Roentgen study of cysticercosis of the central nervous system. *Radiology* **1966**;86:520–528
19. Rabiela-Cervantes MT, Rivas-Hernandez A, Rodriguez-Ibarra J, Castillo-Medina S, Cancino F. Anatomopathological aspects of human brain cysticercosis. In: Flisser A, Willms K, Laclette JP, Larralde C, Ridaura C, Beltran F, eds. *Cysticercosis: present state of knowledge and perspectives.* New York: Academic, **1982**:179–200
20. Grau E, Garrido F, Canedo L. Calcification of the cysticerci of *Taenia solium* in the human brain. In: Flisser A, Willms K, Laclette JP, Larralde C, Ridaura C, Beltran F, eds. *Cysticercosis: present state of knowledge and perspectives.* New York: Academic, **1982**:499–515
21. Slais J. Morphology of the scolex of cysticercus cellulosae in brain cysticercosis. In: Flisser A, Willms K, Laclette JP, Larralde C, Ridaura C, Beltran F, eds. *Cysticercosis: present state of knowledge and perspectives.* New York: Academic, **1982**:235–259
22. Ramirez-Bon E, Merchant MT, Gonzalez-del Pliego M, Canedo L. Ultrastructure of the bladder wall of the metacestode of *Taenia solium.* In: Flisser A, Willms K, Laclette JP, Larralde C, Ridaura C, Beltran F, eds. *Cysticercosis: present state of knowledge and perspectives.* New York: Academic, **1982**:261–280
23. Martinez A. Anatomia patologica de la cisticercosis cerebral. *Neurocirugia* (Santiago) **1961**;19:173–190
24. Escobar A, Nieto D. Parasitic diseases. In: Minckler J, ed. *Pathology of the nervous system*, vol 3. New York: McGraw-Hill, **1972**:2503–2521
25. Trelles JO, Trelles L. Cysticercosis of the nervous system. In: Vinken PJ, Bruyn GW, eds. *Handbook of clinical neurology*, vol 35. Amsterdam: North-Holland, **1978**:291–320
26. Loyo M, Kleriga E, Estanol B. Fourth ventricular cysticercosis. *Neurosurgery* **1980**;7:456–458
27. Gonzalez-Cornejo S. Comment on [43]. *Neurosurgery* **1983**; 12:151–152
28. Willms K. Host-parasite interface in the metacestode of *Taenia solium.* In: Flisser A, Willms K, Laclette JP, Larralde C, Ridaura C, Beltran F, eds. *Cysticercosis: present state of knowledge and perspectives.* New York: Academic, **1982**:397–411
29. Dorfsman J. The radiologic aspects of cerebral cysticercosis. *Acta Radiol [Diagn]* (Stockh) **1963**;1:836–842
30. Taveras JM, Wood EH. *Diagnostic neuroradiology*, 2d ed. Baltimore: Williams & Wilkins, **1976**:222, 224
31. Martinez B (cited in [18]). *Consideraciones sobre la cisticercosis humana* (tesis). Mexico, D.F.: U. of Mexico Medical Library, School of Medicine, **1961**
32. Escobar A. The pathology of neurocysticercosis. In: Palacios E, Rodriguez-Carbajal J, Taveras JM, eds. *Cysticercosis of the central nervous system.* Springfield, IL: Thomas, **1983**:27–54
33. Handler LC, Mervis B. Cerebral cysticercosis with reference to the natural history of parenchymal lesions. *AJNR* **1983**;4:709–712
34. Schultz TS, Ascherl GF Jr. Cerebral cysticercosis: occurrence in the immigrant population. *Neurosurgery* **1978**;3:164–169
35. Brant-Zawadzki M, Bartkowski HM, Pitts LH, et al. NMR imaging of experimental and clinical cerebral edema. *Noninvas Med Imag* **1984**;1:43–47
36. Brasch RC, Weinmann H-J, Wesbey GE. Contrast-enhanced NMR imaging: animal studies using gadolinium-DTPA complex. *AJR* **1984**;142:625–630
37. Mazer S, Antoniuk A, Ditzel LFS, Araujo JC. The computed tomographic spectrum of cerebral cysticercosis. *Comput Radiol* **1983**;7:373–378
38. Zee C-S, Segall HD, Apuzzo MLJ, Ahmadi J, Dobkin WR. Intraventricular cysticercal cysts: further neuroradiologic observations and neurosurgical implications. *AJNR* **1984**;5:727–730
39. Rodriguez-Carbajal J, Palacios E, Azar-Kia B, Churchill R. Radiology of cysticercosis of the central nervous system including computed tomography. *Radiology* **1977**;125:127–131
40. Zee C-S, Segall HD, Miller C, et al. Unusual neuroradiological features of intracranial cysticercosis. *Radiology* **1980**;137:397–407
41. Zee C-S, Tsai FY, Segall HD, Teal JS, Ahmadi J. Entrance of metrizamide into an intraventricular cysticercosis cyst. *AJNR* **1981**;2:189–191
42. Madrazo I, Garcia-Renteria JA, Paredes G, Olhagaray B. Diagnosis of intraventricular and cisternal cysticercosis by computerized tomography with positive intraventricular contrast medium. *J Neurosurg* **1981**;55:947–951
43. Madrazo I, Garcia-Renteria JA, Sandoval M, Lopez-Vega FJ. Intraventricular cysticercosis. *Neurosurgery* **1983**;12:148–152
44. Estanol B, Kleriga E, Loyo M, et al. Mechanisms of hydrocephalus in cerebral cysticercosis: implications for therapy. *Neurosurgery* **1983**;13:119–123
45. Apuzzo MLJ, Dobkin WR, Zee C-S, Chan JC, Giannotta SL, Weiss MH. Surgical considerations in treatment of intraventricular cysticercosis: an analysis of 45 cases. *J Neurosurg* **1984**;60:400–407
46. Guevara-Oropeza M. Tumor del angulo pontocerebeloso. *Arch Neurol Psiquiat* **1938**;1:369–377
47. Bickerstaff ER, Small JM, Woolf AL. Cysticercosis of the posterior fossa. *Brain* **1956**;79:622–634
48. Bustamante A. Lesions of the cerebellopontine angle (excluding neurinomas). *Rev Inst Nal Neurol Mex* **1977**;11:76–81
49. Dublin AB, French BN. Cysticercotic cyst of the septum pellucidum. *AJNR* **1980**;1:205–206